

Hugoniot Equations of State of Several Unreacted Explosives

N. L. COLEBURN AND T. P. LIDDIARD, JR.

U. S. Naval Ordnance Laboratory, Silver Spring, Maryland

(Received 21 June 1965)

JUL 26 1966

Plane shock-wave compressions and an optical method were used to obtain the unreacted equations of state of 11 explosives and propellants for pressures up to 90 kbar. Measurements of the transit times of weak shock waves (~ 100 bar) yielded longitudinal sound-wave velocities.

I. INTRODUCTION

THE dynamic pressure-volume relations, or Rankine-Hugoniot curves, of many solids and several liquids have been measured in recent years. However, fewer data are known for explosives and propellants, because when shocked they readily undergo violent chemical decomposition. This behavior, though, is an important reason for obtaining such data. Any quantitative measurements of shock parameters, used to determine hazards from burning or detonation, require knowing the shock Hugoniot of the unreacted explosive or propellant.

In 1958, Majowicz and Jacobs¹ derived unreacted pressure-volume data from shock experiments using explosive wedges. Their data and the results of Garn² are perhaps the first Hugoniot measurements of unreacted explosive materials. Garn's data are for liquid TNT from 44 to 110 kbar, where chemical reaction begins. Ilyukhin *et al.*³ give shock-wave compression results from 57 to 139 kbar for cast TNT, also pressed RDX and liquid nitromethane.

In this paper⁴ we give the experimentally determined dynamic pressure-volume relations for 11 explosives and propellants. These materials (Table I) include several pure (CHON) explosives⁵ and some plastic-bonded and aluminized mixtures. The pressure-volume relations are derived from optical measurements of the shock-wave and particle velocities. It is assumed that any chemical reaction which began during the shock transit time ($< 1 \mu\text{sec}$) was too small to affect the compression results. Finally, we give the results of extrapolating the shock-wave and particle-velocity data to obtain the so-called von Neumann spike pressure.⁶

II. EXPERIMENTAL METHOD

Dynamic pressure-volume data are derived from shock-wave experiments relating the measured velocities of the shock wave, U_s , and of the material behind

TABLE I. Specimen materials.

Formula or composition	Experimental density (g/cm ³)
2,4,6-Trinitrotoluene (TNT) cast	1.614
1,3,5-Trinitrobenzene (TNB)	1.640
1-Amino-2,4,6-trinitrobenzene (TNA) ^a	1.600
1,3-Diamino-2,4,6-trinitrobenzene (DATB) ^b	1.780
1,3,5-Triamino-2,4,6-trinitrobenzene (TATB)	1.847
60/40 RDX/TNT (Composition B-3) ^c cast	1.680
85/15 HMX/Viton (LX-04-0) ^d	1.879
85/15 HMX/Viton (LX-04-1)	1.863
94/3/3 HMX/nitrocellulose/chloroethyl-phosphate (PBX 9404-03)	1.829
RDX/TNT/Al/Wax	
40/38/17/5 (HBX-1) cast	1.750
31/29/35/5 (HBX-3) cast	1.850
44.76/29.53/20.95/4.76 (H-6) cast	1.760
Propellant ^e (FFP)	1.760
Propellant ^f (EJC)	1.900

^a Zytel (nylon) 5%.

^b Zytel (nylon) 1%.

^c Mixture of 60% cyclotrimethylene trinitramine (RDX) and 40% TNT.

^d Cyclotetramethylene tetranitramine (HMX) 85% and Viton 15%, a fluoro elastomer from DuPont.

^e Plastic composition of ammonium perchlorate and aluminum.

^f Plastic composition of HMX, nitroglycerine, nitrocellulose, ammonium perchlorate, and aluminum.

¹ J. M. Majowicz and S. J. Jacobs, Bull. Am. Phys. Soc., Ser. II 3, 293 (1958).

² W. B. Garn, J. Chem. Phys. 30, 819 (1958).

³ V. S. Ilyukhin, P. F. Pokhil, O. K. Rozanov, and N. S. Shvedova, Soviet Phys.—Doklady 5, 337 (1960) [Dokl. Akad. Nauk SSSR 131, 793 (1960)].

⁴ This work includes additional results from experiments reported at the International Conference on Sensitivity and Hazards of Explosives, London, 1-3 October 1963.

⁵ Explosives composed of carbon, hydrogen, oxygen, and nitrogen only. These materials are pressed except as noted.

⁶ J. von Neumann, OSRD Report No. 549 (1942).

the shock front, u_p , to the pressure P and specific volume V of the compressed material. The relationships are given by the Rankine-Hugoniot equations,

$$V/V_0 = (U_s - u_p)/U_s \quad (1)$$

and

$$P = (1/V_0) U_s u_p \quad (2)$$

The shock-wave velocity in the explosive, or propellant, specimen is obtained from the measured transit

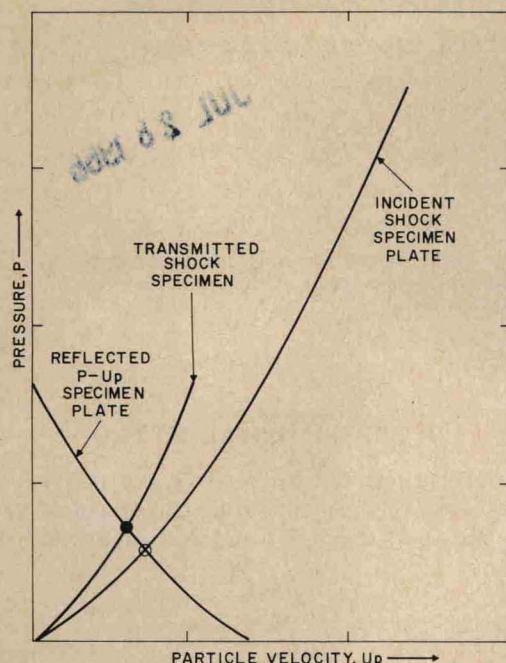


FIG. 1. Graphical solution for particle velocity and pressure in the shocked specimen. ● Specimen, ○ specimen plate.

time of the shock through the specimen. The particle velocity is obtained graphically⁷ using the known Hugoniot for the material on which the specimens were mounted. The latter is referred to hereafter as the "specimen plate." The rarefaction locus is drawn in the P, u_p plane for the specimen-plate material and the shock locus is drawn with slope $(P/u_p) = (1/V_0)U_s$ for the specimen. The point of intersection of the two curves gives the pressure and particle velocity in the specimen. The rarefaction locus is approximated by reflecting the shock Hugoniot for the specimen plate (P -vs- u_p curve, Fig. 1) about the plane which includes the experimental P -vs- u_p point for the specimen-plate material.

III. EXPERIMENTAL ASSEMBLIES

For measurements from 10 to 90 kbar we used the arrangement in Fig. 2. The components consisted of an explosive plane-wave system,⁸ a specimen plate, and several test specimens. The specimens⁹ were formed into short cylinders, ranging from 5 to 13 mm in diameter and 1 to 5 mm in height. (The specimen height was measured to ± 0.003 mm.) The height-to-diameter ratio was generally about 0.1 to 0.3, never greater than 0.5.

⁷ J. M. Walsh, M. H. Rice, R. G. McQueen, and F. L. Yarger, *Phys. Rev.* **108**, 196 (1957).

⁸ J. H. Cook, *Research* (London) **1**, 474 (1948).

⁹ In several experiments, specimen wedges were used. The wedges were of two sizes; 25° with 14-mm apex height, and 30° with 26-mm apex height. See S. J. Jacobs, T. P. Liddiard, Jr., and B. E. Drimmer, *Symp. Combust.* 9th Cornell Univ., Ithaca, N.Y., 1962, 517 (1963).

Typically, with the arrangement of Fig. 2, the shock wave produced by the detonating explosive system arrives at the free surface of a 2.5-cm-thick specimen plate. The arrival is plane parallel to within ± 0.01 μ sec across an 8- to 10-cm diameter. The specimens are placed within this plane region.¹⁰

We varied the pressure transmitted to the specimens in the following ways:

- (1) By changing the composition or thickness of the explosive plane-wave system; e.g., one system uses a 15.8-cm diameter, plane-wave lens to ignite a liquid explosive, nitromethane, of detonation pressure = 102 kbar.
- (2) By changing the composition or thickness of the specimen plate, e.g., brass or Plexiglas.
- (3) By using a shock attenuator composed of alternating layers of high- and low-density materials between the explosive system and test specimens.

Table II gives several typical shock-producing systems.

The shock-wave arrivals at the free surfaces of the specimen plate and the specimens were recorded by a smear camera using a reflected-light technique.¹¹⁻¹³ In this method light is reflected continuously from the free surfaces into the camera. The shock-wave arrival at any point along the surface produces a sudden change in light reflected from that point. The light was provided by two exploding-wire light sources, each composed of a 0.025-mm-diam tungsten wire threaded into a 10-cm-long glass capillary tube. Typically, the energy used to explode the series-connected wires was obtained from the discharge of a 4 μ F capacitor charged to 8 kV. To increase the reflectivity, aluminized Mylar film was placed on the surface of the specimen. The

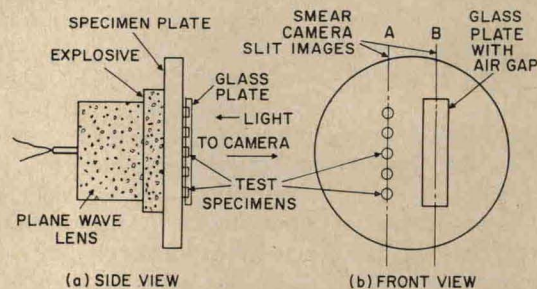


FIG. 2. Arrangement for delivery of plane shock wave and for measuring shock-wave velocities in the specimens and the free-surface velocity of the specimen plate.

¹⁰ A layer of silicone grease about 0.003 mm thick filled the gap between the specimen and the highly polished specimen plate. The specimen was held in place by a small amount of Eastman 910 adhesive placed around the periphery of the specimen.

¹¹ W. A. Allen and C. L. McCrary, *Rev. Sci. Instr.* **24**, 165 (1953).

¹² N. L. Coleburn, Naval Ordnance Laboratory Technical Report, NavWeps Report 6026 (1960).

¹³ T. P. Liddiard, Jr., and B. E. Drimmer, *J. Soc. Motion Picture Television Engrs.* **70**, 106 (1961).

TABLE II. Typical shock-producing systems.

Explosive ^a thickness (cm)	Attenuator thickness (cm)	Specimen-plate thickness (cm)	Pressure ^b (kbar)	Particle velocity ^b (mm/ μ sec)
3.75 CH ₃ NO ₂	...	3.75 brass	200	0.530
3.75 CH ₃ NO ₂	...	2.54 brass	227	0.580
3.75 CH ₃ NO ₂	...	1.27 brass	240	0.613
3.75 CH ₃ NO ₂	0.838 brass/0.838 Plexiglas	0.838 brass	128	0.361
3.75 CH ₃ NO ₂	1.27 brass	2.41 Plexiglas	43.0	0.900
3.75 CH ₃ NO ₂	2.54 brass	2.41 Plexiglas	36.8	0.800
1.27 Comp B	...	2.54 brass	225	0.600
1.27 Comp B	...	1.27 brass	278	0.710
1.27 Comp B	0.838 brass/0.838 hexane	0.828 brass	66.1	0.201

^a Diam 13.9 cm.^b Shock-wave parameters of specimen plate.

aluminized side of the film was held to the specimen surface by an extremely thin layer of silicone grease.

A dual-slit system was used in the camera. The images of the two slits (Fig. 2) were parallel to each other and equally spaced on each side of the center of the specimen plate. Usually one slit was aligned across the test specimens, the other being used to record the free-surface motion of the specimen plate. A glass "flasher" plate, mounted a small (but accurately known) distance from the specimen-plate surface, was used to obtain the free-surface velocity.

The various shock-producing systems (Table II) were calibrated by using free-surface-velocity measurements of specimen plates and the corresponding shock-wave velocities obtained from the known equations-of-state of specimen-plate materials.¹⁴ The calibrations were checked and refined by frequently including samples of the specimen-plate material in the same experiments with the explosive specimens. The shock transit times within the specimens were determined from the intensity changes occurring in the reflected light when the shock wave arrived at the free surface.¹⁵ These times were divided into the specimen heights to obtain mean shock-wave velocities. By this method we obtained the U_s -vs- u_p relations for naval brass and Plexiglas, as well as for the explosive specimens. Naval brass is nominally composed of 59.00% Cu; 0.50%–1.00% Sn; 0.4% maximum impurity; and the remainder, Zn. For the brass (density = 8.37 g/cm³),

$$U_s(\text{mm}/\mu\text{sec}) = 3.560 + 1.833u_p, \quad (3)$$

and for Plexiglas,

$$U_s(\text{mm}/\mu\text{sec}) = 2.710 + 1.568u_p - 0.037u_p^2. \quad (4)$$

Measurements of the transit times of weak shock waves (~ 100 bar) were used to obtain "sound" wave

¹⁴ The free-surface velocity for a plane shock wave is almost twice the particle velocity. See R. W. Goranson, D. Bancroft, B. L. Burton, T. Blechar, E. E. Houston, E. F. Gittings, and S. A. Landeen, *J. Appl. Phys.* **26**, 1472 (1955); J. M. Walsh and R. H. Christian, *Phys. Rev.* **97**, 1544 (1955).

¹⁵ See N. L. Coleburn, *J. Chem. Phys.* **40**, 71 (1964) for the description and analysis of a typical record obtained using the reflected-light technique.

velocities¹⁶ in larger specimens, 1.27 cm thick by 5.08-cm diameter. In the experiment (Fig. 3) a cylinder (or slab) of the explosive is immersed in a Plexiglas aquarium. A detonator is centered 30 cm from the plane surface of the specimen. The initiation of the detonator produces a shock wave in water which is nearly plane when it arrives at the surface of the specimen. The motion of the shock wave is recorded by a smear camera using a shadowgraph technique; i.e., backlighting with collimated light from an exploding wire. The resulting record (Fig. 4) permits measuring the transit time of the shock wave in the specimen and the shock-wave velocity in the water before and after the wave enters the specimen.

IV. RESULTS

Figures 5, 6, 7, and 8 are plots of the experimental measurements of shock-wave and particle velocities in

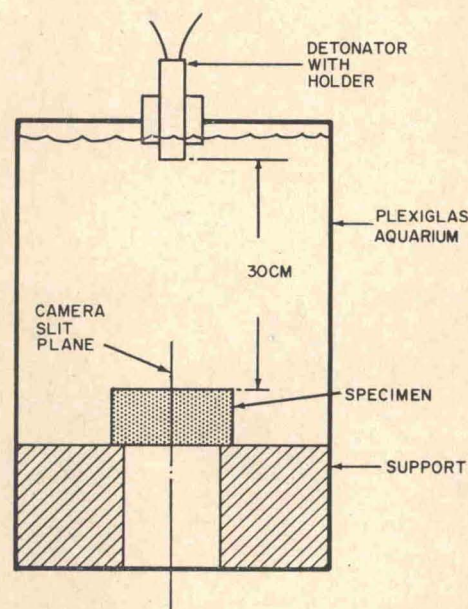


FIG. 3. Arrangement for initiating and measuring weak shock waves (~ 100 bar).

¹⁶ J. M. Majowicz, Naval Ordnance Laboratory Technical Report, NavOrd Report 4524 (1957), classified.

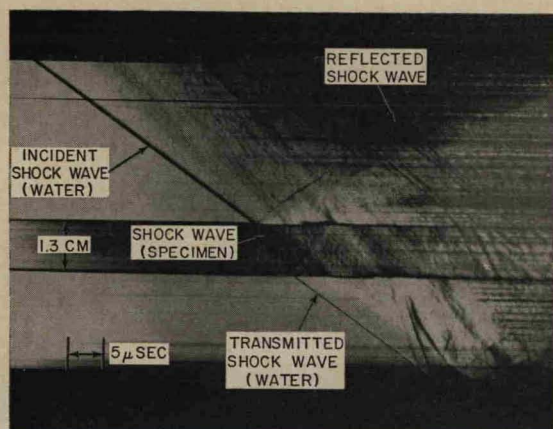


FIG. 4. Smear-camera shadowgraph of shock waves obtained using the arrangement of Fig. 3. The upper and lower traces are from the incident and transmitted shock waves in water. The central dark band denotes the specimen height. The shock trace in the specimen (Plexiglas) is seen within this band.

the CHON explosives. The measurements for the aluminized explosives and propellants are plotted in Fig. 9. The data show that the shock-wave velocity is a linear function of the particle velocity within experimental error over a wide range, i.e.,

$$U_s = A + Bu_p \quad (5)$$

from particle velocities of about 0.3 to 1.2 mm/μsec.

If Eq. (5) applies to the lower amplitude limit, $u_p = 0$, and the behavior of the material is fluidlike,

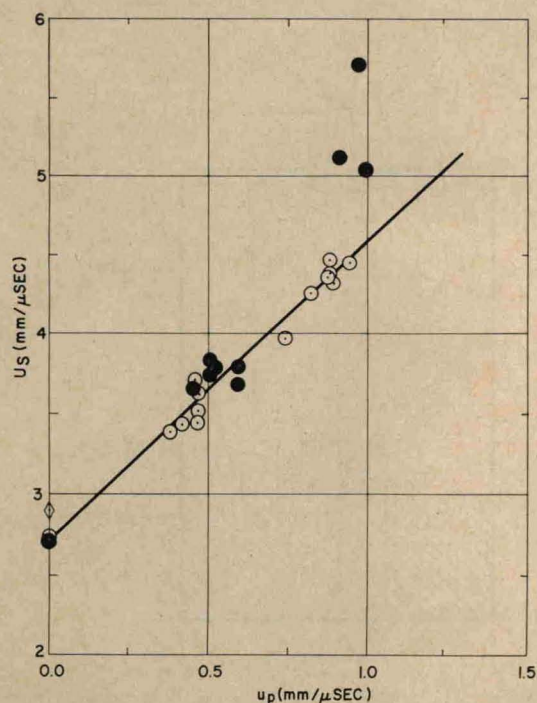


FIG. 5. Shock-wave velocity, U_s , vs particle velocity, u_p , of Composition B-3 (○), LX-04-0 (●). [PBX 9404-03 (◇), sound velocity included for comparison.]

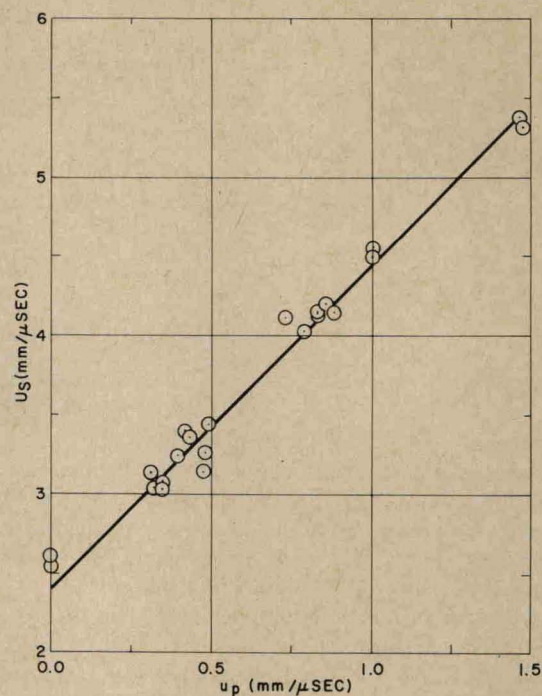


FIG. 6. Shock-wave velocity, U_s , vs particle velocity, u_p , on TNT.

then according to theory the intercept A should equal the adiabatic bulk-sound speed. Our first thoughts were that the weak-shock-velocity experiments should give good approximate values of the bulk velocities. By

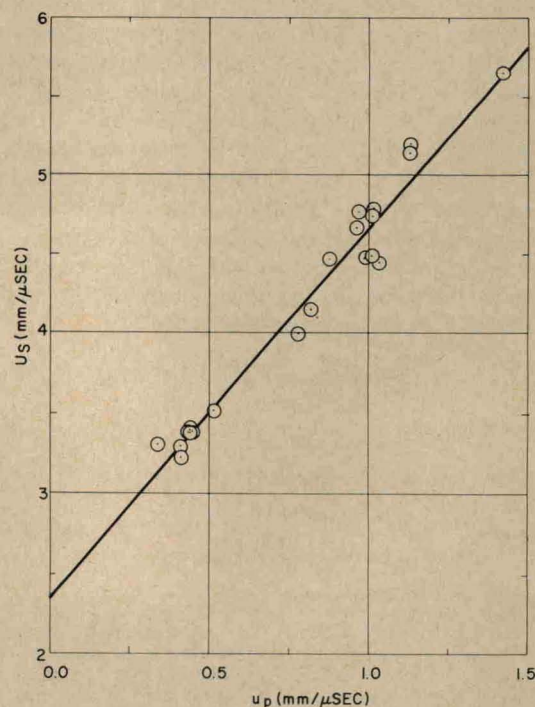


FIG. 7. Shock-wave velocity, U_s , vs particle velocity, u_p , of TATB.

using piezoelectric (tourmaline) gauges in the weak-shock experiments, we measured an incident water shock pressure of 60 bar and calculated pressures ranging from 80 to 100 bar with small particle flow (~ 5 m/sec) in the explosives. The measurements at this point were made close to the elastic limit. The explosives usually were recovered from these experiments unchanged, although several were cracked by the shock. Measurements in several plastics indicate the velocities of these weak shocks essentially are those of longitudinal sound waves.¹⁷⁻¹⁹ These are 10%-30% greater than the bulk sound velocities calculated from elastic constants. Since data on sound velocities in explosives are scarce,²⁰ the

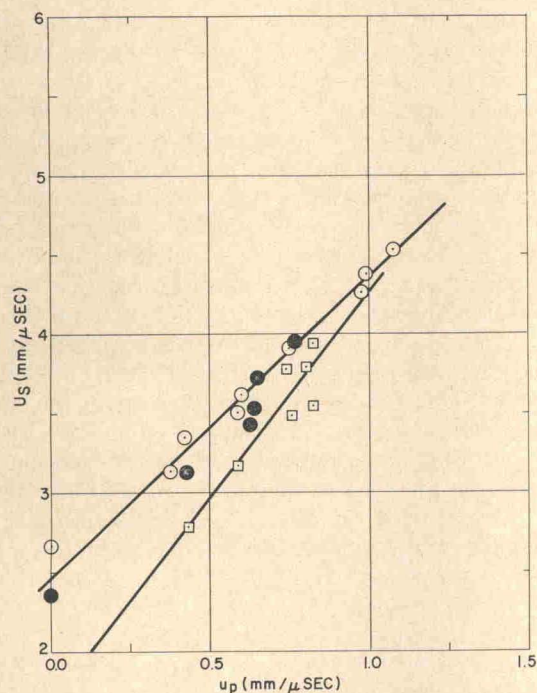


FIG. 8. Shock-wave velocity, U_s , vs particle velocity, u_p , of DATB (○), TNB (●), and TNA/Zytel (□).

longitudinal wave velocities, obtained from the weak-shock measurements, are listed in Table III.

The weak-shock values are shown at $u_p=0$ in the U_s -vs- u_p diagrams for comparison with the higher-am-

¹⁷ For Plexiglas, e.g., we measured a wave velocity of 2760 m/sec. The reported longitudinal sound velocity is 2770 m/sec.¹⁸ The incident and transmitted shock-wave velocities in the water were 1492 and 1490 m/sec. The precise sound velocity is 1481.63 m/sec¹⁹ in distilled water at 20°C.

¹⁸ M. Auberger and J. S. Rinehart, J. Appl. Phys. **32**, 219 (1961).

¹⁹ W. D. Wilson, J. Acoust. Soc. Am. **31**, 1067 (1959).

²⁰ For comparison with sound velocity of TNT obtained from ultrasonic measurements, see L. Aronica, Naval Ordnance Laboratory Report 6087 (1961); J. B. Ramsay and A. Popolato, "Analysis of Shockwave and Initiation Data for Solid Explosives," Symposium on Detonation, 4th, U.S. Naval Ordnance Laboratory, Silver Spring, Maryland, October 1965; R. J. Wasley and J. F. O'Brien, "Low Pressure Hugoniot of Solid Explosives," Symposium on Detonation, 4th, U.S. Naval Ordnance Laboratory, Silver Spring, Maryland, October 1965.

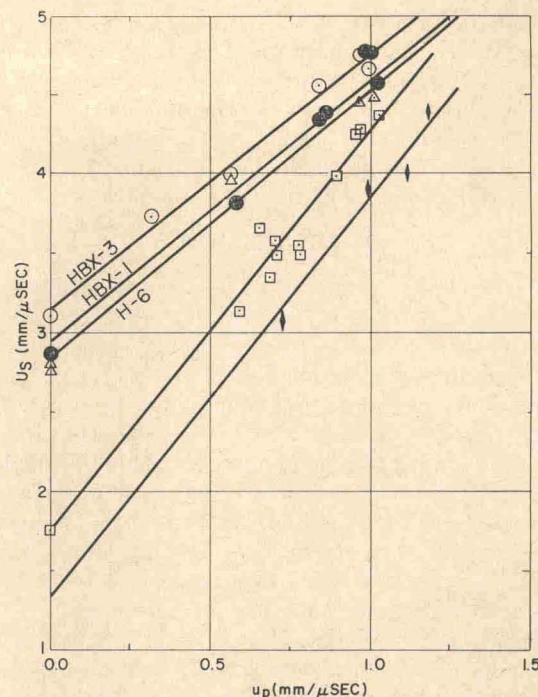


FIG. 9. Shock-wave velocity, U_s , vs particle velocity, u_p , of several aluminized explosives and propellants. ○ HBX-3, ● HBX-1, △ H-6, □ EJC, ◆ FFP.

plitude shock-wave measurements. However, they were not included in the linear treatment of the U_s -vs- u_p data.²¹ Consequently, few shock-wave data were obtained for $u_p < 0.3$ mm/μsec, and the linearity of the lower region of the shock-velocity-particle-velocity curve is not fully established. Also, the possibility may

TABLE III. Equation-of-state constants.

Explosive	Longitudinal sound velocity [(cm/sec) × 10 ³]	A ^a [(cm/sec) × 10 ³]	B ^a
TNT	2.572	2.390 ± 0.032	2.050 ± 0.034
Composition			
B-3	2.736	2.710 ± 0.046	1.860 ± 0.065
TATB	2.050	2.340 ± 0.065	2.316 ± 0.076
DATB	2.660	2.449 ± 0.043	1.892 ± 0.058
TNB	2.356	2.318 ± 0.072	2.025 ± 0.123
TNA	...	1.700 ± 0.243	2.531 ± 0.337
EJC	1.760	1.724 ± 0.147	2.550 ± 0.183
FFP	...	1.327 ± 0.148	2.430 ± 0.146
HBX-1	2.860	2.936 ± 0.078	1.651 ± 0.095
HBX-3	3.095	3.134 ± 0.017	1.605 ± 0.024
H-6	2.759	2.832 ± 0.068	1.695 ± 0.083
PBX 9404-03	2.919
LX-04-1	2.539
LX-04-0	2.688

^a A and B are the intercept and slope, respectively, of the shock-velocity-particle-velocity curve.

²¹ Where only several data were obtained, e.g., H-6, the weak shock velocity was included.

exist of the presence of elastic precursor waves in the explosives at low amplitudes. Therefore, any extrapolation of the data to particle velocities much below 0.3 mm/ μ sec perhaps is not justified. Table III, though, lists the sound velocities and the constants A and B with their probable errors as determined from the weighted data by the method of least squares.

V. DISCUSSION

The sources of experimental error are: shock-wave curvature ($\pm 0.01 \mu$ sec), uncertainty in record analysis (0.1% to 0.5% of U_s , depending on record quality), specimen density variation ($\pm 0.002 \text{ g/cm}^3$), and effects of chemical reaction on the velocity measurements. The latter errors were minimized by the following means (1) The velocity measurements were made in cylinders with heights of only 1–5 mm; and (2) the experiments reported here were limited to transmitted pressures below 90 kbar. At a given input pressure the maximum height of each specimen depended upon the shock sensitivity of the particular explosive sample.

In practice the maximum specimen height was set by the length of run over which the shock wave has a reasonably constant initial velocity as measured in wedge-test experiments.²² The wedge test differentiates between explosives by the ease with which chemical reaction is initiated and grows from shock impact. The growth of chemical reaction produces an increase in the shock-wave velocity for increasing explosive thickness. The onset of chemical reaction is dependent upon the amplitude and duration of the shock. For pressures below 90 kbar in 25° wedges (apex angle 90°), 14-mm apex height, the velocity of the shock in most of the materials showed no significant increase within the first 5 mm of travel. In several insensitive explosives no velocity increase was measured in much greater shock transit distances, e.g., at 60–70 kbar, TATB (>14 mm) and cast TNT (8 mm). Both of the latter explosives display initial constant velocities for distances longer than 5 mm with shocks of 100 kbar or more. The above precautions eliminated all experiments in which gross buildup of reaction would be present. The possibility of weak reaction behind the transmitted shock must still be considered.

In the wedge-test experiments the shock wave cannot be a true square step. Therefore, one would expect that rarefactions would cause such shocks to decay with distance of travel. In two experiments with TATB the decay was observed. The failure to decay in other experiments could be due to energy being fed into the shock front by chemical reaction. However, in the region of initial constant velocity it is very unlikely that reaction effects could exactly balance rarefaction effects to achieve steady velocities for relatively long

periods. It is more likely that the shock velocity is not a sensitive function of pressure.

Majowicz and Jacobs²² have indicated that the transition from pure shock to detonation in cast solids may involve an induction period before chemical reactions begin, as inferred from the region of constant shock velocity. (The existence of induction periods in liquid explosives and explosive single crystals is generally accepted.) However, Cachia and Whitbread,²³ also Campbell, Davis, Ramsay, and Travis,²⁴ conclude that even for small shock amplitudes the transmitted shock in polycrystalline explosives is accelerating, and initiates a small amount of chemical reaction in certain regions with essentially no delay.

It is possible, of course, that isolated sites of chemical reaction have resulted from the sudden impact even at the lowest pressures of our experiments. If so, during the shock transit times ($< 1 \mu$ sec) such reactive sites might be expected to contribute only to a small degree, perhaps 1%–2% or less, to the energy of the shock. Since the shock-velocity-particle-velocity relations are linear for many nonreactive solids, a linear behavior for the explosives given here is a significant indication that our measurements are essentially free of reaction effects. If appreciable chemical reaction occurred during any compression experiment, its energy contribution would cause the shock to accelerate.²⁵ This, typically, would be indicated by an abrupt increase in the slope of the U_s -vs- u_p curve and perhaps by luminous traces on the smear-camera records. Both the acceleration of U_s and the presence of luminosity were obtained for the plastic-bonded explosive LX-04-0. As seen in Fig. 5, the data at about $u_p = 0.5 \text{ mm}/\mu\text{sec}$ are in line with that of cast Composition B-3. At about $u_p = 0.8 \text{ mm}/\mu\text{sec}$ and above, though, the LX-04-0 specimens were obviously reacting, whereas for Composition B-3 there apparently is little reaction at this shock level. PBX 9404-03 reacted too readily to give any unreacted data even at the lower pressures. Incidentally, cast rather than pressed TNT was used in our experiments since the latter also reacts too fast to give reliable unreacted Hugoniot data much above 20 kbar.

The usual experimental error in measuring dynamic compressibilities, where no reaction is possible, is about 5%. We, therefore, consider that the deviations caused by reaction in our explosive specimens are not enough to affect appreciably the unreacted compression results in this spread of error, except where noted. The probable mean-square errors of $\pm 59 \text{ m/sec}$ in U_s and $\pm 33 \text{ m/sec}$ in u_p for Composition B-3 are typical of the data. These results lead to a probable relative error of $\pm 6.7\%$

²² G. P. Cachia and E. G. Whitbread, *Proc. Roy. Soc. (London)* **A246**, 268 (1958).

²⁴ A. W. Campbell, W. C. Davis, J. B. Ramsay, and J. R. Travis, *Phys. Fluids* **4**, 498 (1961).

²⁵ S. J. Jacobs, T. P. Liddiard, Jr., and B. E. Drimmer, *Symp. Combust. 9th Cornell Univ., Ithaca, N.Y., 1962*, 517 (1963).

²² J. M. Majowicz and S. J. Jacobs, *Naval Ordnance Laboratory Report 5710* (1958).

in pressure (at 30.6 kbar) when Composition B-3, for example, is compressed to 86% of its original volume.

The experimental Hugoniot, from Eqs. (1), (2), and (5) is

$$P = A^2(V_0 - V) / [V_0 - B(V_0 - V)]^2, \quad (6)$$

and the bulk modulus is

$$-V \frac{dP}{dV} = \frac{-A^2(V/V_0) \{1 + B[1 - (V/V_0)]\}}{V_0 \{1 - B[1 - (V/V_0)]\}^3}. \quad (7)$$

The compressibility coefficients, computed from Eq. (7), are diagramed in Fig. 10 as a function of decreasing

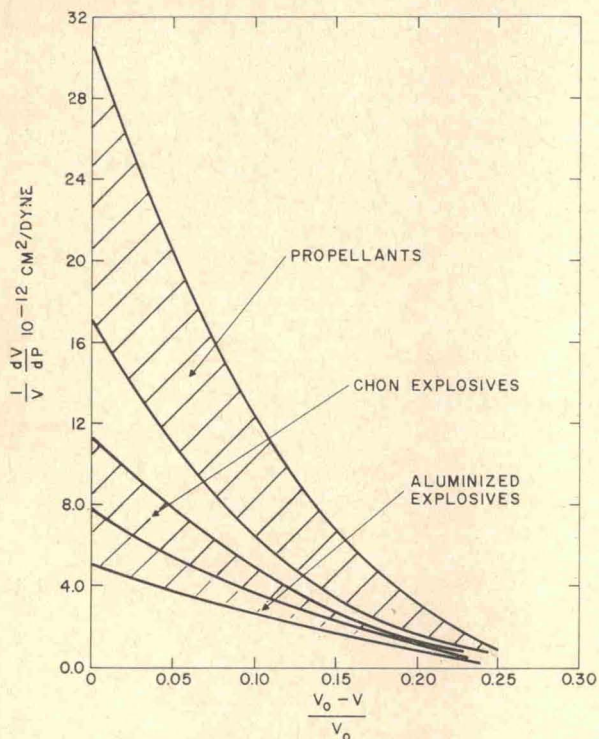


FIG. 10. Compressibility vs relative volume of CHON explosives, aluminized explosives, and propellants.

specific volume (increasing pressure). The two curves of lowest initial compressibility, $(1/V_0)(dV/dP)$, $(5 \text{ to } 8 \times 10^{-12} \text{ cm}^2/\text{dyn})$ show the range of data for the aluminized explosives HBX-1, HBX-3, and H-6. All solid CHON explosives with initial densities $\geq 98\%$ of crystal density probably are within the range of the second set of curves. Composition B-3, e.g., has an initial compressibility of $8.1 \times 10^{-12} \text{ cm}^2/\text{dyn}$; TNT, $10.9 \times 10^{-12} \text{ cm}^2/\text{dyn}$; and TNB, $11.3 \times 10^{-12} \text{ cm}^2/\text{dyn}$. The composite and double-base propellants are easily compressed and form the upper range of data with initial compressibility coefficients of $17 \text{ to } 31 \times 10^{-12} \text{ cm}^2/\text{dyn}$.

Finally, it is of interest to determine the peak (spike) pressures ahead of the detonation front in the explosives according to von Neumann's theory. We have obtained

TABLE IV. Detonation parameters of several explosives.

Explosive	$P(\text{spike})$ (kbar)	P_{C-J} (kbar)	D (mm/ μsec)
TNT	237	189	6.81
TNT ^a	327	210	6.99 ^b
Composition B-3	382	283	7.95
DATB	336	251	7.60
TATB	340	259	7.66
H-6	360	245	7.40
HBX-3	370	206	7.53
TNA	235	176	7.00
TNB	307	219	7.27

^a See Ref. 3.

^b See Ref. 28.

these pressures by a linear extrapolation of the U_s -vs- u_p data and the assumption that our U_s -vs- u_p relations represent nonreactive Hugoniot to the detonation velocities of the explosives. The P -vs- V/V_0 curves obtained from the extrapolation show the complete shock Hugoniot for the unreacted explosive, if one assumes that the linear U_s -vs- u_p relation holds all the way up to the spike pressure. On the basis of von Neumann's model of a plane detonation, the intersection of this

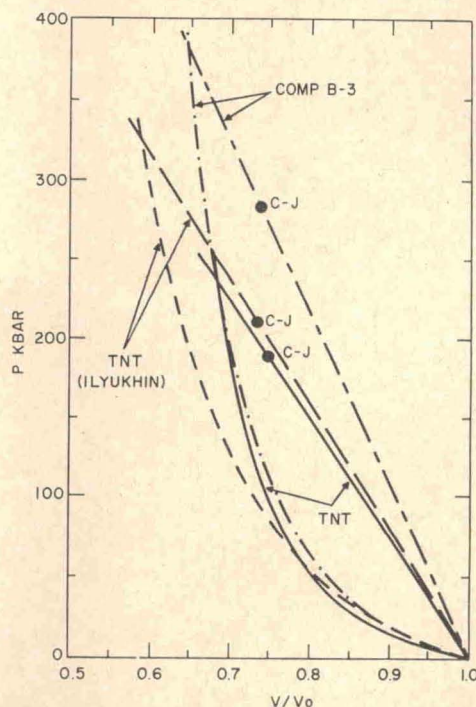


FIG. 11. The shock Hugoniot for nonreacting TNT and Composition B-3, extrapolated to the von Neumann spike pressure.

Hugoniot curve with the Rayleigh line²⁶ will yield the von Neumann spike pressure. The Rayleigh line is the straight line on the P -vs- V/V_0 plane, of slope $-\rho_0 D^2$, passing through the point (0, 1). (D is the steady-state detonation velocity of the explosive.) By means of this procedure the spike pressures listed in Table IV were obtained.

Our data show that the spike pressure exceeds the Chapman-Jouguet (C-J) pressure,²⁷ e.g., by 35% in Cast Composition B-3, and by 25% in Cast TNT. However, the second set of TNT data, Ilyukhin,³ gives a spike pressure some 55% greater than 210 kbar, the pressure considered correct by Ilyukhin for the C-J

²⁶ The conservation relations, Eq. (1) and (2), yield the equation $P = \rho_0 U_s^2 [1 - (V/V_0)]$. von Neumann's analysis shows that the straight line on the $P, V/V_0$ plane satisfying this equation (the Rayleigh line), where U_s is replaced by D , intersects the shock Hugoniot of the unreacted explosive at the spike pressure point.

²⁷ N. L. Coleburn, Naval Ordnance Laboratory Technical Report 64-58 (1964).

point. Despite the differences²⁸ in P_{C-J} (and D), the principal discrepancy in the two sets of data is due to the differences in the measurement of the dynamic compressibility of TNT as shown in the Hugoniot curves of Fig. 11. This discrepancy indicates a need for further refinement in the experimental techniques in order to increase the accuracy of such measurements.

ACKNOWLEDGMENTS

The authors are indebted to J. Schneider and W. A. Brown for their careful assistance in the experiments. Of considerable help were the many stimulating discussions with B. E. Drimmer, S. J. Jacobs, and D. Price.

²⁸ Ilyukhin's data were obtained with *cast* TNT. The D value he used is that of *pressed* TNT. See M. J. Urizar, E. James, Jr., and L. C. Smith, *Phys. Fluids* **4**, 262 (1961). Our data indicate that the detonation velocities of *pressed* and *cast* TNT are statistically different for equal initial densities < crystal density (1.654 g/cm³). However, the differences in detonation velocities do not account for the discrepancy between Ilyukhin's value and our value for the spike pressure of TNT.